Quantification of Myocardial Muscarinic Receptors with PET in Humans

Jacques Delforge, Dominique Le Guludec, André Syrota, Bernard Bendriem, Christian Crouzel, Michel Slama and Pascal Merlet

Service Hospitalier Frédéric Joliot, Commissariat à l'Energie Atomique, Orsay, France; Service de Médecine Nucléaire, Hôpital Bichat, Paris, France; and Service de Cardiologie, Hôpital Béclère, Clamart, France

The potential for noninvasive quantification of myocardial muscarinic receptors using PET data, a mathematical model, multi-injection protocols and ^{11}C-labeled methylquinuclidinyl benzilate (MQNB) as a radioligand was previously demonstrated in dogs. The present study examines the possibility of optimizing the experimental protocol to make this approach suitable for human studies. For six normal subjects, the protocol included three injections: a tracer injection, followed 30 min later by an injection of an excess of unlabeled MQNB (displacement) and then 30 min later by a simultaneous injection of unlabeled and labeled MQNB (coinjection). The model input function was estimated from the PET data corresponding to the left ventricular cavity. This protocol enables a separate evaluation of all parameters of a ligand-receptor model which includes three compartments and seven parameters. The complexity of this three-injection protocol, however, appears to be inconvenient for clinical use. A simplified two-injection protocol (tracer injection and coinjection) was evaluated in five other normal subjects and the results were compared to those obtained with the three-injection protocol. In regions of interest over the left ventricle, the mean value of the receptor concentration B'_{max} and the equilibrium dissociation constant K_d were 26 ± 7 pmole/ml tissue and 2.0 ± 0.5 pmole/ml tissue, respectively. The possible existence of nonspecific binding was studied in two subjects using a double-displacement protocol. The corresponding rate constant was found to be very low (0.03 min^{-1}).

J Nucl Med 1993; 34:981–991

The potential for quantification of myocardial muscarinic receptors in vivo using positron emission tomography (PET), a mathematical model, multi-injection protocols and ^{11}C-labeled methylquinuclidinyl benzilate (MQNB) as a ligand was previously demonstrated in dogs (*1*). The advantage of this methodology is that it provides the ability to quantify receptor concentration noninvasively. This advantage was recently discussed (*2*) along with the practical difficulties of this study due to the complexity of the mathematical models and the experimental protocol used (arterial blood sampling, four injections, injection of a large amount of unlabeled ligand, 3-hr experiment). The present study examines the possibility of optimizing the experimental protocol to make this multi-injection approach suitable for human studies.

Muscarinic cholinergic receptors in balance with beta-adrenergic receptors play a key role in the regulation of the rate and force of heart contractions. Changes in receptor number and affinity have been reported in physiological, pharmacological and clinical conditions in animal models as well as in humans (*3–11*). The development and use of radioligands with high affinity and specificity to the muscarinic receptor have greatly contributed to the knowledge of receptor biochemistry (*12*). Tritium-labeled antagonists, such as quinuclidinyl benzilate (QNB), atropine, dexetimide, N-methyl-scopolamine (NMS) or N-methylatropine, have been shown to bind to an equal number of sites with Hill coefficients close to unity. This indicates that these antagonists bind to a single class of high affinity binding sites (*13–16*). The noninvasive quantification of muscarinic receptor may be of value in investigating possible changes in receptor number and/or affinity, especially after pharmacological intervention or during the follow-up of patient with heart disease. PET now allows the measurement of both labeled ligand concentration within the myocardium and its variations (*17,18*). Measurements are made using a specifically synthetized radioligand, in most cases a selective receptor antagonist labeled with a positron-emitting isotope such as ^{11}C or ^{18}F.

MQNB, the quaternary derivative of QNB, is a nonmetabolized and, contrary to QNB, hydrophilic antagonist. Therefore, the portion not extracted by the lungs binds only to cell surface receptors. It possesses, like QNB, a high affinity and specificity for cholinergic receptors in rat heart homogenates (*19,20*). Its binding is stereospecific since the pharmacologically active isomer, dexetimide, can displace ^{11}C-MQNB from its binding sites, whereas the inactive isomer, levetimide, remains inactive (*19*).

However, knowledge of the ligand concentration given by PET does not allow receptor concentration to be directly deduced. It is necessary to use a mathematical model which describes ligand-receptor interactions whose parameters (which include receptor concentration) have to

Received Aug. 24, 1992; revision accepted Feb. 2, 1993.
For correspondence or reprints contact: Jacques Delforge, PhD, Service Hospitalier Frédéric Joliot, 4 Place du Général Leclerc, 91406 Orsay, France.

be identified from the kinetic curves in a dynamic PET experiment. The model used here has four compartments and seven parameters. A unique and accurate identification of such a large number of parameters from a single experimental data set requires a multi-injection approach (*1,21*). Three kinds of injections are possible: an injection of labeled ligand with high specific activity (so that the percentage of receptors occupied is very small after such an injection), an injection of unlabeled ligand (the percentage of receptors occupied after such injection can be large if a high amount of ligand is injected) or a mixture of labeled and unlabeled ligand (which corresponds to an injection of labeled ligand with low specific activity). Obviously, these last two choices are possible only if administration of a high amount of ligand does not induce a pharmacological effect.

The choice of a protocol for clinical investigation requires minimizing radioactivity doses, using low unlabeled ligand doses and limiting the duration of the experiment. The first protocol used included three successive injections: a tracer injection, an injection of an excess of unlabeled MQNB and a coinjection of unlabeled and labeled MQNB. With this protocol, a separate evaluation of all parameters was possible (*1*). However, the complexity of this protocol limits its use in human investigations. Because a single injection is insufficient for estimating receptor concentration (*21*), the possibility of identifying parameters from data obtained only by a two-injection protocol was examined. By using an "experimental design optimization" method (*22*), the experimental protocol was optimized (types of injection, time of injection, injected doses) in order to obtain the best possible estimation of receptor concentration from the acquired data.

MATERIAL AND METHODS

Preparation of ^{11}C-MQNB

MQNB was labeled with high specific radioactivity using ^{11}C by methylation of QNB with ^{11}C-methyl iodide (*19*). Labeled material, with a specific radioactivity varying from 300 to 1200 mCi/μmole at the time of injection, was purified using high-performance liquid chromatography.

Subjects

Thirteen normal healthy volunteers, mean age 32 ± 6 yr (range 24–44 yr), were studied. They were free of any cardiac disease on the basis of clinical, ECG and echocardiographic examinations, and none were taking medication. The acquisition protocol was applied early in the morning on fasting subjects. For a subset of three volunteers, a 5Fr catheter was percutaneously placed into the radial artery once the quality of their cubital pulse and collateral function was checked clinically. During the study, arterial blood pressure was measured twice: before the transmission scan and 60 min after the last MQNB injection. Heart rate was continuously monitored and the ECG was recorded every minute for 5 min after each injection and every 5 min between each sequence. Written informed consent was obtained from each subject. The study protocol was approved by the Ethics Committee of our institution.

PET Measurements

PET studies were performed using a seven-slice time-of-flight assisted positron camera (*23*) (LETI TTV03, Commissariat à l'Energie Atomique, Grenoble, France). In this instrument, each slice is 9 mm thick and the spatial transverse resolution is about 7 mm. Transmission scans are obtained with a rotating ^{68}Ge source to correct emission scans for the attenuation of 511 keV photon rays through the body thorax. Emission data are recorded in list mode starting with the first injection of ^{11}C-MQNB until the end of the experiment. Between 50 and 75 sequential images, using one of the seven cross-sections, were reconstructed according to the specific experimental protocol used for each patient.

Experimental Protocols

Three kinds of experimental protocols were used in three distinct subsets of subjects.

Three-injection Protocol. A PET study with the complete protocol including three injections of ^{11}C-MQNB and/or MQNB was performed on six normal subjects. At the beginning of the experiment, about 10 mCi (e.g., 370 MBq) of ^{11}C-MQNB was intravenously injected over a period of about 1 min. The corresponding dose of radioactive tracer was denoted by J_0^* (from 4 to 10 μg). Thirty minutes later, a second intravenous injection of an excess of unlabeled ligand (amount J_1 from 0.2 to 0.4 mg) was administered. Sixty minutes after the beginning of the experiment a third injection, consisting of a mixture of labeled (about 8 mCi) and unlabeled MQNB in the same syringe, was administered ("coinjection" experiment). The injected quantities of labeled and unlabeled ligand are denoted by J_2^* (from 13 to 37 μg) and J_2 (from 0.2 to 1 mg), respectively. The total experiment lasted 90 min. Exact doses administered to each subject are given in Table 1.

Coinjection Protocol. For five subjects, a coinjection protocol was used, including only an initial tracer injection followed 30 min afterwards by a simultaneous injection of labeled and unlabeled MQNB (from 8 to 22 μg and from 0.15 to 0.4 mg, respectively). The total experiment took 70 min.

Double-displacement Protocol. For two subjects, a three-injection protocol was used which involved, after initial tracer injection, two injections of unlabeled MQNB (0.3 mg) at 30 min and 60 min, respectively. The entire experiment lasted 90 min.

Image Analysis

One set of sequential images, corresponding to one of the seven cross-sections that intersected the left ventricule, was selected for the analysis. The outer myocardial boundary was automatically defined by an isocontour plotting routine. The 70% isocontour, which was selected on a 10-min image, included the septum and the left ventricular wall.

List mode acquisition allowed the time-of-flight confidence-weighted reconstruction of 10-sec images during the first 2 min following labeled ligand injection and longer duration images (up to 5 min) when radioactivity slowed down. Radioactivity was measured in each region of interest (ROI) after correction for ^{11}C decay and was expressed as pmole/ml after normalization using the specific radioactivity measured at time 0. When the protocol included two injections of labeled ligand, all ^{11}C-MQNB was produced by the same synthesis and the specific radioactivity measured at time 0 was then identical in both injections.

Calibration was performed every week with a cylindrical phantom containing a uniform source of ^{68}Ge. Myocardial wall thickness was measured by echocardiography and PET data were corrected for count recovery loss. This was due to the small size of the heart wall when compared to the spatial resolution of PET.

TABLE 1
Numerical Values of the Protocol Parameters Corresponding to the Experiments Performed on Six Subjects Using a Complete Protocol

	Subj. 1	Subj. 2	Subj. 3	Subj. 4	Subj. 5	Subj. 6	Units
Inj. durat.*	1	0.25	1	1	0.45	1	min
Spec. activ.†	717	358	450	534	1119	911	mCi/μM
Initial injection (time 0)							
J_0^*	5.2	10.5	8.8	7.9	4.2	4.1	μg
Displacement (at 30 min)							
J_1	0.25	0.4	0.4	0.2	0.3	0.3	mg
Coinjection (at = 60 min)							
J_2^*	22.7	34.6	37.2	19.4	13.0	15.3	μg
J_2	1	0.4	0.4	0.2	0.3	0.3	mg
Experiment duration: 90 min							

*Duration of injections, which was approximately identical for all injections corresponding to an experiment.
†Specific activity measured at time 0.
The doses J_i^* correspond to labeled ligand and the doses J_i to unlabeled ligand.

The correction was performed using a recovery factor measured experimentally on a heart phantom with the same PET system. The end-diastolic thickness of the ventricular septum of the left ventricle was measured by echography and was found to be 9.6 ± 0.6 mm. The ratio of true-to-measured concentration was equal to 0.67 for a 9.6-mm thickness in the phantom calibration experiments. Spillover from blood cavity to myocardium was not corrected but was accounted for through a vascular fraction (F_V, see the ligand-receptor model section) that was fitted.

Plasma Radioactive Concentration Measurements

The identification of model parameters necessitated knowledge of the plasma time-concentration curve $C_a^*(t)$ which was used as the input function in subsequent modeling. To avoid the necessity of arterial blood samples, comparisons were made in three subjects between the PET concentration obtained using a ROI in the left ventricular cavity and the concentration obtained with arterial blood samples (about 0.4 ml) collected from the radial artery. The time interval between each arterial sample varied. Samples were taken every 5 sec for 2 min after injections of labeled MQNB. The sampling interval was increased to 10 min when blood radioactivity slowed. Carbon-11 radioactivity was measured after rapid centrifugation in a gamma counting system (Kontron CG 4000) and time-activity curves were corrected for physical decay of ^{11}C activity from time 0. Arterial concentrations were expressed as pmole/ml plasma after division by the specific radioactivity.

The Ligand-Receptor Model

The compartmental model used in this study and shown in Figure 1 is a nonequilibrium nonlinear model (*1,24*). The flux of nonmetabolized free ligand from compartment 1 to compartment 2 is given by $pV_RC_a^*(t)$ (as pmole/min/ml tissue). $C_a^*(t)$ is the plasma concentration of labeled ligand at time t, p is a rate constant (as ml/min/ml) and V_R (as ml/ml) is defined as the fraction of the ROI delineated by PET in which the ligand can react with receptors. With a hydrophilic ligand, V_R is likely to correspond approximately to the fraction of extracellular fluid. The quantity of labeled free ligand present in the interstitial volume (compartment 2) (pmole/ml tissue) is M_f^*. The free ligand could bind directly to a free receptor site, bind irreversibly to a nonspecific site or escape with rate constant k. The specific binding probability depends on the bimolecular association rate constant (k_{+1}) and on the local concentration of free receptor sites equal to $[B'_{max} - M_b^*(t)]$. B'_{max} is the unknown quantity of receptor sites available for binding and $M_b^*(t)$ is the quantity of labeled ligand bound to receptors in 1 ml of myocardium. The irreversible nonspecific binding probability of the free ligand is denoted by k_{ns} and the rate constant for the dissociation of the bound ligand by k_{-1}.

This model contains six parameters, the two most important being the concentration of receptor sites available for binding B'_{max} and the ratio of k_{-1} to k_{+1} to define the equilibrium dissociation constant K_d.

The protocols previously described include injections of unla-

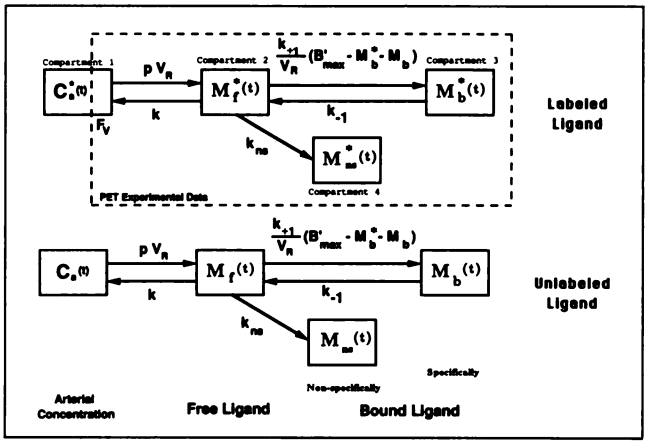

FIGURE 1. Compartmental ligand-receptor model used in analysis of myocardial tissue data obtained after intravenous injection of ^{11}C-MQNB. The upper part represents the model describing labeled ligand kinetics (quantities denoted by an asterisk) and the lower part the same model associated with the unlabeled ligand. Compartment 1 represents blood, compartment 2 free ligand, compartment 3 specifically bound ligand and compartment 4 irreversibly nonspecifically bound ligand. All transfer probabilities of ligand between compartments are linear except for binding probability which depends on the bimolecular association rate constant and on local concentration of free receptor sites. PET experimental data correspond to the sum of the labeled ligands in compartments 2, 3 and 4 and of a fraction F_V of compartment 1. The unlabeled ligand compartments are not directly observable from PET data, but the concentration of specifically bound ligand ($M_b(t)$) has an effect on the local concentration of free receptors and consequently on the binding probability of free labeled ligand.

beled ligand during displacement and coinjection experiments. Thus, unlabeled ligand kinetics affect the local concentration of free receptors and must be taken into account. Free unlabeled ligand is denoted by $M_f(t)$, specifically bound unlabeled ligand by $M_b(t)$ and nonspecifically bound unlabeled ligand by $M_{ns}(t)$, which are expressed as pmole/ml tissue. Unlabeled ligand kinetics were assumed to be similar to those of the labeled ligand and the two parts of the model associated with the labeled and unlabeled ligand respectively have the same structure and parameters. Plasma concentrations of unlabeled ligand ($C_a(t)$) were calculated by simulation using the curve $C_a^*(t)$ which corresponds to labeled ligand (*22*). It is assumed that blood curves have a similar shape and are proportional to the mass injected for each separate injection. A comparison of the blood curves after tracer injection and after coinjection justifies this assumption (see doses in Table 1).

In PET studies, experimental data acquired between time t_{i-1} and time t_i are given by the following integral relation:

$$M_T^*(t_i) = \frac{1}{t_i - t_{i-1}} \int_{t_{i-1}}^{t_i} (M_f^*(t) + M_b^*(t) + M_{ns}^*(t) + F_V C_b^*(t))\, dt, \quad \text{Eq. 1}$$

where $C_b^*(t)$ is the whole blood time-concentration curve and F_V is a parameter identified with the other model parameters. F_V represents fractional volume, including both the fraction of blood present in the tissue volume and the effect of spillover from blood cavity to myocardium.

The model parameters are identified by minimization of the usual weighted least squares cost function and estimation of the standard errors is based on the use of the covariance matrix and the residual value of the cost function (*1,25*).

RESULTS

The protocol experiment was well tolerated in all subjects. Four of the six subjects who had the three-injection protocol complained of slight mouth dryness.

Blood Time-Concentration Curve and Model Input Function

Blood concentration measurements shown in Figure 2 correspond to those of experiment 1. After each injection of labeled ligand (which took about 1 min to perform), blood concentration increased rapidly and reached a maximum within 30 sec at the end of the injection. Figure 2 also shows blood concentration estimates obtained from PET data with a ROI in the left ventricular cavity. A good agreement between the two measurement methods is observed. Similar results were obtained with two other subjects. The labeled MQNB blood concentration could be used to the model input function since it had been verified that this molecule is not metabolized and that the plasma-to-blood ratio is constant during the duration of the experiment (*1*). Therefore, this PET estimation of the model input function is justified. Interestingly, this method has the main advantage of avoiding arterial blood sampling in patients.

Myocardial Time-Concentration Curves

Figure 3 shows an example of experimental data obtained with a three-injection protocol (experiment 1 in Table 1). After the initial tracer injection of [^{11}C]MQNB,

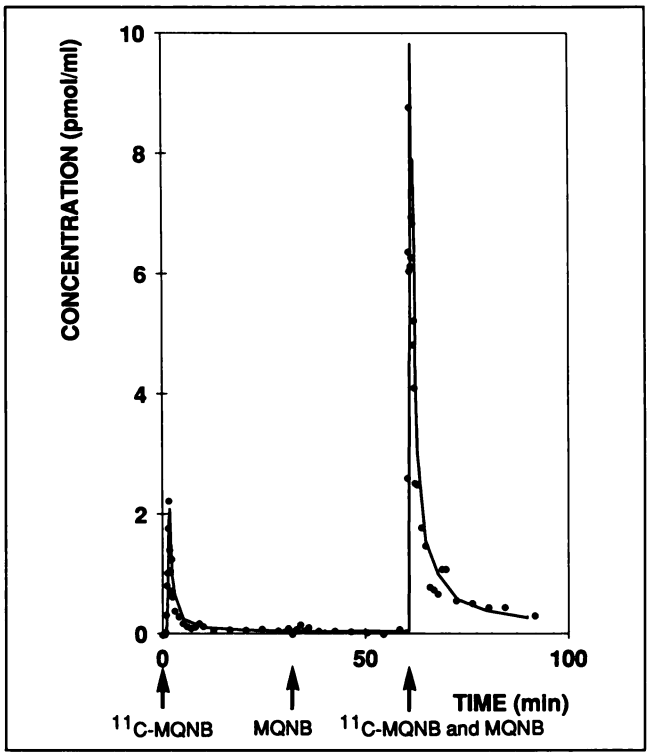

FIGURE 2. Comparison between the two methods for measuring blood time-concentration curves. The solid line shows the curve obtained by blood sampling, whereas the solid circles give the concentrations estimated using a PET ROI in the left ventricular cavity. This curve demonstrates the good agreement between the two methods. The two peaks corresponding to the injections of labeled ligand (at 0 and 60 min) are easily observable. The injection of unlabeled ligand (at 30 min) resulted in small peaks of radioactivity due to dissociation of labeled bound ligand. Exact timing and doses are given in Table 1 (experiment 3) and in the legend of Figure 3.

myocardial concentration increased rapidly and after 10 min remained constant until displacement (at 30 min). The injection of unlabeled MQNB resulted in a decrease in myocardial concentration, which reflects the dissociation of labeled bound ligand. However, the percentage of the displacement (about 70%) is lower than the percentage previously observed in dogs (*1*) because the injected amount of MQNB did not allow complete occupancy of the receptor sites. Coinjection of labeled and unlabeled MQNB at 60 min produced a fast peak in the myocardial time-concentration curve, which contrasted with the plateau observed when labeled ligand was injected alone.

Parameter Identification

A fit of the mathematical model to the myocardial PET experimental data provided values for kinetic rate constants and receptor densities (Table 2). In these results, nonspecific binding was neglected, and thus the parameter k_{ns} was assumed to be null. The final quality of the fits was satisfactory (Fig. 3). If a new parameter, such as a nonspecific binding rate constant, was included in the model, this would lead to unidentifiable parameters. An estimate of the standard error was obtained for each identified parameter. This value was estimated using the covariance matrix and

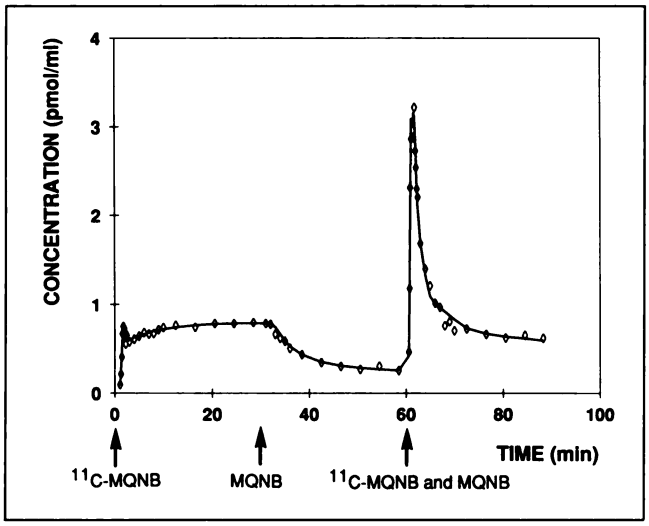

FIGURE 3. Three-injection protocol with tracer injection at time 0, injection of unlabeled ligand at 30 min and coinjection at 60 min. A comparison is made between the experimental PET data (open diamonds) (experiment 1) and the model simulation (solid line). Corresponding model parameter values are shown in Table 2, column 1.

the residual value of the least squares cost function (*1,25*). Mean parameter values and standard deviations were calculated for the six subjects. The mean receptor density was 26 ± 7 pmole/ml tissue and the product K_dV_R was 0.30 ± 0.08 pmole/ml tissue. It should be noted that the relative standard errors estimated for each subject corresponded only to the influence of the differences between model-predicted concentrations and the experimental data. Therefore, they did not include the influence of various uncertainties, such as individual variability, uncertainties about specific activity and instrumentation errors. This explains why the standard errors were often lower than the usual standard deviations on B'_{max} mean values.

Computer Simulation

Myocardial time-concentration curves for the free, bound and total ligands were calculated by using the parameter values given in Table 2. Figure 4 shows the result of the simulation obtained with the parameters estimated from experiment 1. The concentration measured with PET is the sum of the ^{11}C-MQNB concentrations in the free and bound ligand compartments and in the vascular fraction of the myocardium within the ROI. Computer simulations showed that most of the radioligand was specifically bound to receptor after injection at a high specific activity (between 0 and 30 min). After the first displacement, the concentration of specifically bound ligand remained higher than that of other compartments. The dissociation rate constant k_{-1} was the limiting parameter in the dissociation of bound ^{11}C-MQNB after displacement (at 30 min). Prior to coinjection of ^{11}C-MQNB and MQNB at 60 min, the percentage of free ligand was less than 1%. Rapidly after the coinjection, all receptors were occupied by unlabeled ligand so that the concentration of free labeled ligand increased quickly and became larger than bound labeled ligand concentration for a short period. The bound ligand concentration, however, remained preponderant at the end of the experiment.

Two-Injection Protocol

The complexity of the three-injection protocol can be inconvenient and so simplification of it was examined. The first injection of a multi-injection protocol is always a tracer injection of labeled ligand. It is well known that identifying receptor concentration implies at least two injections, one of which results in ligand occupation of a significant percentage of receptor sites. Thus, the second injection has to include a large amount of unlabeled ligand. Two types of two-injection protocols (coinjection and displacement) are possible, depending on whether or not the second injection includes a tracer dose of labeled ligand.

The displacement protocol is the simplest of the two, but a previous study in dogs (*1*) showed that identification of the parameters from data obtained using such a protocol leads to two different solutions and thus provides two distinct sets of parameter values that fit the experimental data with the same statistical quality. The same study showed

TABLE 2
Individual Model Parameters from MQNB Data in Six Normal Subjects Using the Protocols Described in Table 1

Parameters (units)	Parameter estimates ± standard errors*						
	Subj. 1	Subj. 2	Subj. 3	Subj. 4	Subj. 5	Subj. 6	Mean ± s.d.†
pV_R (min^{-1})	0.29 ± 0.02	0.29 ± 0.02	0.42 ± 0.02	0.34 ± 0.02	0.41 ± 0.03	0.28 ± 0.03	0.34 ± 0.06
k (min^{-1})	1.7 ± 0.2	1.2 ± 0.1	2.2 ± 0.3	1.8 ± 0.4	4.5 ± 2.0	2.6 ± 1.1	2.3 ± 1.1
k_{+1}/V_R (ml/(pmole · min))	1.4 ± 0.8	1.5 ± 0.5	1.5 ± 0.4	1.5 ± 0.6	0.9 ± 0.4	1.2 ± 0.6	1.33 ± 0.22
k_{-1} (min^{-1})	0.45 ± 0.20	0.23 ± 0.03	0.33 ± 0.03	0.36 ± 0.09	0.25 ± 0.05	0.43 ± 0.02	0.34 ± 0.08
B'_{max} (pmole/ml)	35.7 ± 1.5	20.1 ± 0.9	19.6 ± 0.8	18.2 ± 1.1	34.4 ± 1.5	27.9 ± 1.7	26.0 ± 7.0
F_V	0.29 ± 0.03	0.35 ± 0.02	0.46 ± 0.04	0.76 ± 0.04	0.54 ± 0.03	0.50 ± 0.04	0.48 ± 0.14
K_dV_R‡ (pmole/ml)	0.37 ± 0.04	0.18 ± 0.03	0.25 ± 0.05	0.27 ± 0.05	0.31 ± 0.14	0.43 ± 0.14	0.30 ± 0.08

*Standard errors calculated using the covariance matrix (*1*).
†Usual standard deviations calculated from the six experiments.
‡$K_d = k_{-1}/k_{+1}$.

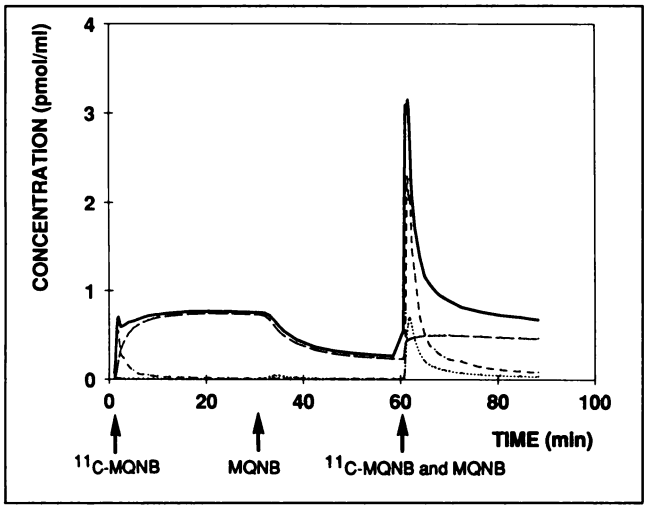

FIGURE 4. Simulation corresponding to experiment 1 (see Fig. 3). The solid line represents simulated experimental data consisting of the sum of the concentrations of the two extravascular compartments and the vascular fraction of blood (including the effect of spillover from the blood cavity). The dotted line corresponds to free ligand concentration (compartment 2), the dashed line to specific binding (compartment 3) and the short dashed line to the vascular fraction.

how easy it is to distinguish the biologically correct solution by comparing the values of the parameters k and k_{-1} (*1*). The results obtained in humans confirm those obtained in dogs, which indicate that the biologically valid solution is the solution in which k_{-1} is lower than k. Both protocols can lead to a unique solution, but the coinjection protocol has the advantage of leading directly to that solution.

To set up the best protocol, the experimental design optimization method was used (*22*). In most situations, there are a number of variables in the experimental protocol that can be chosen. It has been proven that a judicious selection of sampling times, injected ligand doses and other degrees of freedom can have a significant effect on parameter estimate uncertainties. Figure 5 shows the coefficient of variation on B'_{max} as a function of unlabeled ligand dose used in coinjection and displacement protocols. This simulation is based on the model parameters obtained with the three-injection protocol (Table 2) and the coefficients of variation have been calculated with a relative data standard deviation equal to 1% (*22*). Figure 5 shows that the smallest uncertainty on B'_{max} obtained using a coinjection protocol is two times smaller than the best value obtained with the displacement protocol. However, the most important result is that this small uncertainty is obtained with the coinjection protocol by using only 0.2 mg of unlabeled ligand dose, whereas the best result with the displacement protocol implies the use of about 1 mg. Taking into account the influence of the unlabeled ligand dose on heart rate (discussed later), this result is a strong argument in favor of the coinjection protocol.

Table 3 shows the model parameter estimates obtained with five subjects using the coinjection protocol. Figure 6 gives an example of an experimental curve and of the corresponding fitting result. A comparison with the results from the three-injection protocol (Table 3) shows that receptor concentration estimation is not significantly altered by simplification of the protocol.

Nonspecific Binding Effect

In the previous study in dogs (*1*), a four-injection protocol showed a nonspecific binding process which appeared irreversible during the experiment. Because such a protocol is unsuitable for humans, we studied possible nonspecific binding in two subjects using a double-displacement protocol. This protocol was chosen using the following experimental design consideration: to allow an increase in the percentage of nonspecific binding in the PET concentration at the end of the experimental curve. Figure 7 corresponds to one of these two studies and shows myocardial PET data (symbol) and fitting results obtained from the mathematical model including (solid line) or not including (dotted line) irreversible nonspecific binding (parameter k_{ns}). The final quality of the fits appears satisfactory only if irreversible nonspecific binding is included in the model. The k_{ns} values identified from the two experiments were 0.029 ± 0.011 min^{-1} and 0.033 ± 0.023 min^{-1}, respectively.

This parameter was not identifiable from the three-injection protocol because the corresponding fits are good without it. To estimate, however, the errors resulting from this neglected parameter, all three-injection protocol curves were fitted to the model, including irreversible nonspecific binding whose corresponding parameter k_{ns} is not fitted and is set to 0.031 min^{-1} (the mean of the two estimated values using the double-displacement protocol). Table 3 also shows the model parameter estimates obtained using this method.

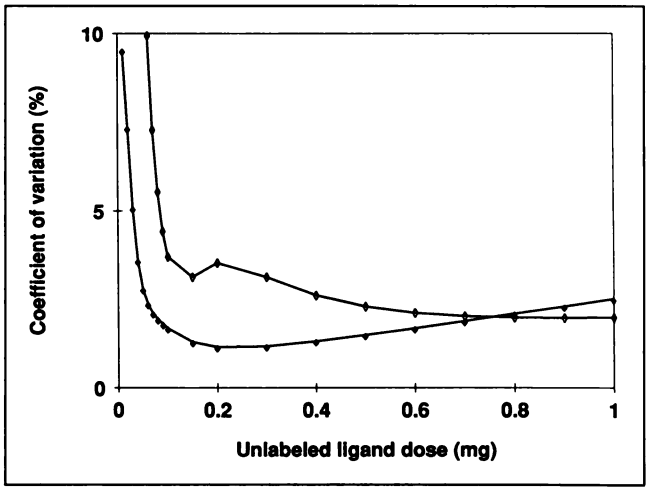

FIGURE 5. Effect of the amount of unlabeled dose used during a coinjection experiment (closed diamonds) or a displacement experiment (open diamonds) on the coefficient of variation of receptor concentration estimates. These simulations were made with parameter values obtained from the complete protocol (Table 2) and a data coefficient of variation set to 1% (*22*). For other values, the relative parameter standard deviation was obtained by the product of the coefficient of variation with the estimate of the data relative standard deviation expressed as a percentage.

TABLE 3
Comparison Between the Model Parameters Identified from MQNB Data Obtained with Different Conditions

Protocol	Coinjection (n = 5)	Three-injection protocol (n = 6)		
Correction parameters (units)	Without	Without	Nonspecific*	Nonspecific* + heart rate†
		Parameter estimates ± standard deviations‡		
pV_R (min^{-1})	0.46 ± 0.10	0.34 ± 0.06	0.37 ± 0.08	0.37 ± 0.07
k (min^{-1})	3.9 ± 1.7	2.3 ± 1.1	2.3 ± 0.7	2.4 ± 0.5
k_{+1}/V_R (ml/(pmole · min))	1.6 ± 1.4	1.3 ± 0.2	1.6 ± 0.6	1.7 ± 0.7
k_{-1} (min^{-1})	0.29 ± 0.24	0.34 ± 0.08	0.26 ± 0.14	0.29 ± 0.13
B'_{max} (pmole/ml)	25 ± 7	26 ± 7	22 ± 6	20 ± 6
F_V	0.41 ± 0.10	0.48 ± 0.14	0.55 ± 0.10	0.53 ± 0.17
K_dV_R§ (pmole/ml)	0.36 ± 0.38	0.30 ± 0.08	0.23 ± 0.14	0.20 ± 0.11

*Nonspecific binding was not identifiable from this protocol, and these results correspond to identified parameters obtained by setting the value of k_{ns} to 0.031 min^{-1}, the average of the values identified from the two double-displacement experiments.
†Parameter values obtained by using corrections of heart rate variations described in the text.
‡Usual standard deviations calculated from six experiments (three-injection protocol) or from five experiments (coinjection protocol).
§$K_d = k_{-1}/k_{+1}$.

The parameter k_{ns} is small and simulations show that with the three-injection protocol the percentage of nonspecifically bound ligand, when compared to the PET measured concentration, was less than 0.7% at 1 min and increased to 3% at 60 min and to 17% at the end of experiment. This last percentage decreases with the unlabeled ligand dose and it was always less than 8% with the coinjection protocol.

Heart Rate Variations and Their Influence on the Estimated Parameters

For the six three-injection experiments, the baseline heart rate was 69 ± 12 bpm and remained unchanged after tracer injection. The injection of unlabeled ligand (0.31 ± 0.07 mg) at 30 min resulted in a slight heart rate increase (74 ± 17 bpm). After the coinjection (including an injection of 0.43 ± 0.26 mg of unlabeled MQNB), heart rate increased within the 5 min following the third injection to a maximum at 10 min (98 ± 13 bpm) and persisted until the end of the procedure.

In the five coinjection experiments, the baseline heart rate was 74 ± 6 bpm and coinjection at 30 min (including 0.25 ± 0.08 mg of unlabeled ligand) resulted in a slight increase in heart rate (78 ± 7 bpm).

Heart rate variations result in blood flow variations and consequently in pV_R parameter variations. Therefore, it is

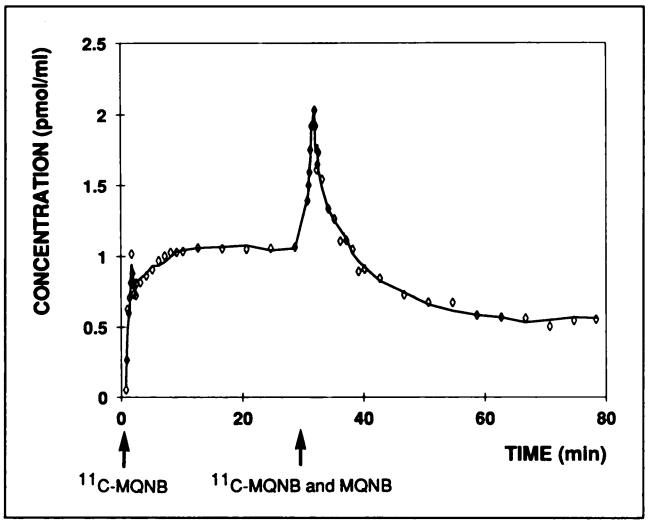

FIGURE 6. Coinjection protocol with tracer injection at time 0 (6.5 μg of ^{11}C-MQNB with a specific activity of 826 mCi/μM) and injection of labeled and unlabeled ligand at 30 min (8.3 μg and 0.2 mg of MQNB, respectively). A comparison is made between the experimental PET data (open diamonds) and the model simulation (solid line).

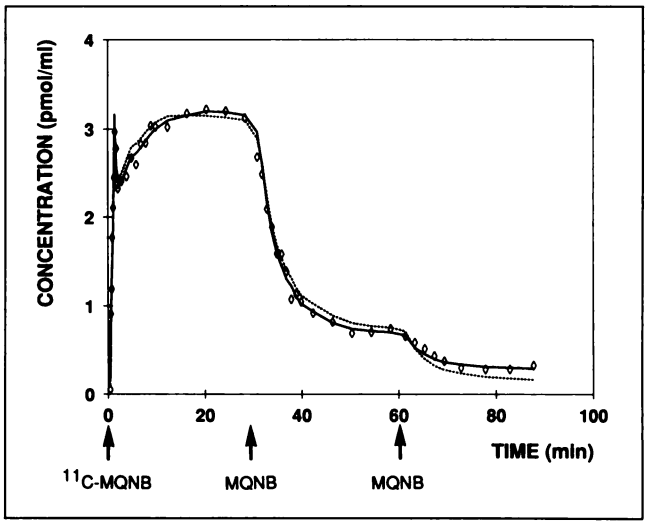

FIGURE 7. Double-displacement experiment with two injections of 0.3 mg of MQNB at 30 and 60 min, respectively. A comparison is made between the experimental PET data (open diamonds) and the fitting result obtained with (solid line) or without (dotted line) nonspecific irreversible binding. The fit is clearly the best and makes it possible to estimate k_{ns}.

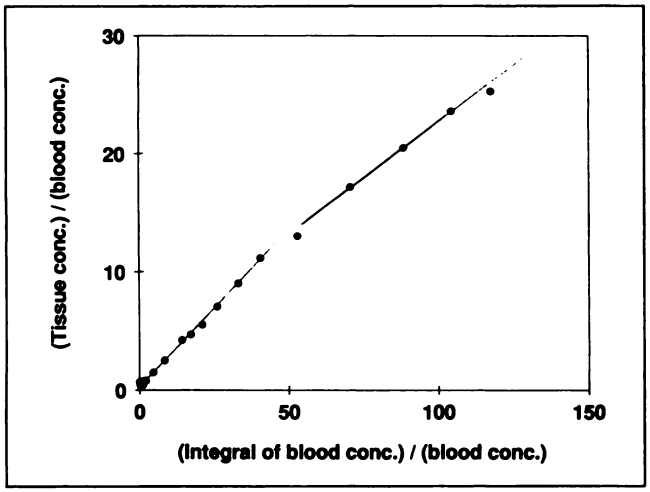

FIGURE 8. Normalized graphical plot used in analysis of myocardial tissue data obtained after injection of ^{11}C-MQNB. The ratio of tissue-to-blood concentration at time t was plotted versus normalized time, defined as the integral of blood concentration from time 0 to t divided by blood activity at time t, according to the method first proposed by Patlak. This figure was generated with data from study 1 (see Table 1) that corresponds to tracer injection (0–30 min) only.

important to estimate the relationship between baseline heart rate and the parameter pV_R. However, the use of the identified parameters pV_R (Table 2) for such a study is open to criticism because they have been identified with the hypothesis that they were constant during the experiments, whereas heart rate was significantly increased after the third injection. Thus, pV_R corresponding to baseline heart rate was estimated using the normalized graphical method or the Patlak plot (*26*). The ratio of tissue-to-blood concentrations at time t was plotted versus "normalized time," defined as the integral of blood concentration from time 0 to t divided by the blood concentration at time t. This graphical method was applied only on the first part of the experimental curves resulting from the tracer injection which were similar regardless of the protocol used.

Figure 8 shows the normalized graphical plot corresponding to study 1 of Tables 1 and 2. The initial slope corresponds to the parameter pV_R, and the slope of the final linear portion of the curve has been used by some authors to estimate k_3, the classical notation of (k_{-1}/V_R) B'_{max}. Similar to the result from the dog study (*1*), it can be seen that the order of magnitude of the final slope (0.209 min^{-1}) does not correspond to the order of magnitude of k_3 (50 min^{-1}), but corresponds to that of pV_R (0.29 min^{-1}). The initial slope (0.295 min^{-1}) gives the exact value of pV_R identified with the fitting method. The difference between the initial and final slope corresponds to the influence of binding reversibility.

This graphical method of estimating the parameter pV_R has been applied to all 13 tracer injection curves. The corresponding baseline heart rates ranged from 52 to 80 bpm. Figure 9 shows that the initial slope of the Patlak plot and thus the parameter pV_R increases almost linearly with heart rate. Assuming that extrapolation of this linear relationship to higher values of heart rate (from 80 bpm to 110 bpm) is valid, the influence of heart rate variations on identified parameters was tested by imposing the constraint that pV_R varies similarly to heart rate (HR). That is, at each time t, the model sets $pV_R(t) = (pV_R)_{baseline} * HR(t)/(HR)_{baseline}$. The results corresponding to the three-injection protocol are given in Table 3, where the pV_R value is the estimate of $(pV_R)_{baseline}$. A comparison with the third column in the same table allows us to conclude that heart rate variations have an effect on parameter estimates, but that this effect is not significant when compared to the magnitude of standard deviations.

DISCUSSION

It is now possible to characterize different cardiac receptors using antagonists of muscarinic, beta-adrenergic or peripheral-type benzodiazepine receptors labeled with positron-emitting isotopes (*17,20,27*). However, a method for quantitatively measuring these receptors is required to investigate possible alterations in heart disease. PET enables the direct measurement of labeled ligand concentration in a ROI, but does not directly measure receptor concentration, which requires a dynamic series of images and a mathematical model.

The model for in vivo ligand-receptor interactions includes at least two steps. First, transport of the ligand from the blood compartment to a free ligand compartment. Second, a classical ligand-receptor interaction that is similar to that used for in vitro studies. Thus, the mathematical model includes at least five to eight parameters and the estimation of such a number of parameters is only possible with complex protocols which seem unsuitable for human studies. Usually, some hypotheses are introduced in order to simplify the model (such as equilibrium hypotheses), or the receptor concentration variation is studied using indexes theoretically correlated with receptor concentration.

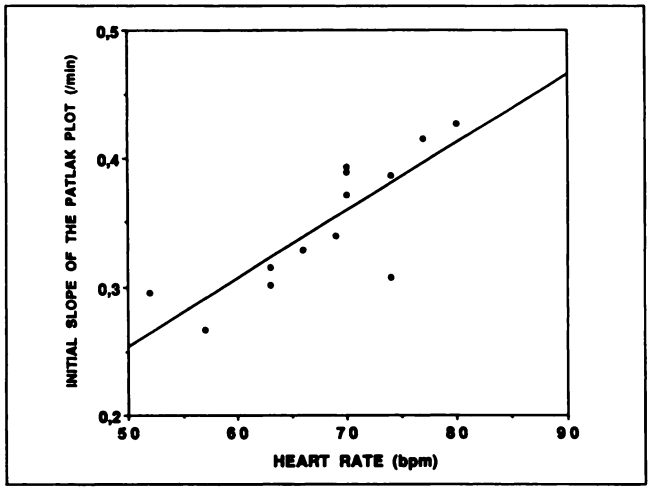

FIGURE 9. Influence of the heart rate on the initial slope of the Patlak plot. This initial slope directly gives pV_R, which is related to blood flow. Each symbol (black square) corresponds to one of the 13 experiments (only the first part of the curve corresponding to tracer injection was used). The straight line is the fit with a linear curve ($y = -0.011 + 0.0052\ x$).

It is true that these sorts of hypotheses can be useful because they often provide a way of estimating receptor concentration variations. However, validation of these hypotheses is often difficult and leads to doubtful results. For example, it has been shown with MQNB that binding of the labeled ligand is not limited by receptor concentration but by the transfer from the blood compartment to the free ligand compartment. This indicates that the normalized graphic method is not suitable for estimating receptor concentration variations and that myocardial PET images obtained after a single tracer injection would be a map of myocardial blood flow rather than an actual map of receptor distribution (*1,2*).

We suggest that determination of a justified quantification method implies two steps: (1) a preliminary study in animals using complex protocols to provide consequent information about ligand kinetics and (2) a simplification of the model and an optimization of the protocol for human studies based on hypotheses justified by preliminary animal study results. Quantification of muscarinic receptors using MQNB as a ligand is the first example of this approach. The preliminary study demonstrated that PET quantification of muscarinic receptors in dogs using a four-injection protocol was possible (*1*). The present study was undertaken to evaluate the possibility of estimating receptor concentration in humans using only a two-injection protocol.

The present results show that a complete protocol, including three injections, allows all parameters of the model to be estimated in humans. From these parameters and use of an experimental design optimization procedure, it is possible to set up an optimized two-injection protocol to allow accurate identification of receptor concentration. Besides the fact that the coinjection protocol has some inconveniences (chemists have more manipulations and the radiation dose absorbed by the patient is doubled), it appears more feasible than the displacement protocol for estimating receptor concentration. In particular, this estimation is possible with a coinjection protocol using an unlabeled ligand dose with no significant effect on heart rate.

A comparison between the results from the three-injection protocol and the coinjection protocol (Table 3) shows that the experimental design optimization procedure was successful since individual uncertainty about receptor concentration as well as the mean values of receptor concentration are not altered by simplification of the protocol. The quantity of receptor sites available for in vivo binding (B'_{max}) estimated by the model was found to be 26 ± 7 pmole/ml tissue with the three-injection protocol and 25 ± 7 pmole/ml tissue with the two-injection protocol. The two estimates are equal with a probability level of 0.87. This value was calculated using the detailed results for B'_{max} estimates (see Table 2 for the three-injection protocol results; the values corresponding to the two-injection protocol are 20.9 ± 1.2, 23.0 ± 1.7, 20.2 ± 1.8, 23.0 ± 4.8, 38.7 ± 2.2 pmole/ml). These results are comparable to those obtained in dogs either in vivo [42 ± 11 pmole/ml tissue (*1*)] or in vitro with ^{3}H-QNB by our laboratory [8.6 ± 0.9 pmole/g tissue or 105 ± 5 pmole/g protein (*1*)] or by other authors (11 pmole/g tissue (*14*) and 242 pmole/g protein (*28*), which corresponds to about 19.8 pmole/g tissue by taking into account the protein-to-tissue ratio measured in our laboratory). This last value is very close to the estimate of muscarinic receptor concentration obtained in humans by using ^{3}H-QNB [275 pmole/g protein (*29*)].

Simplification of the protocol, however, led to a poorer estimation of all other parameters. For example, the K_dV_R mean value determined using the three-injection protocol was 0.30 ± 0.08 pmole/ml tissue, whereas the value obtained with the two-injection protocol was 0.36 ± 0.38 pmole/ml. The latter mean value obtained in five subjects appeared consistent with the mean value obtained using the complete protocol, but the large standard deviation observed with the two-injection protocol shows that the individual values of K_dV_R may be without real significance. Individual estimates obtained for the five subjects were 0.20 ± 0.20, 0.19 ± 0.16, 0.29 ± 0.09, 0.06 ± 0.06, 1.08 ± 0.23 pmole/ml, respectively. This comment applies in varying degrees to all the other model parameters except for B_{max}. This is an indication that the coinjection protocol, with chosen doses of unlabeled MQNB, was well optimized to estimate receptor concentration. However, the estimate of K_dV_R found by this multi-injection approach is close to the value obtained in humans by using ^{3}H-QNB [0.58 pmole/ml (*29*)].

The volume of reaction V_R is not identifiable from the PET data. Because MQNB is a very hydrophilic molecule, V_R can be considered close to the fraction of extracellular fluid estimated at 0.15 ml/ml tissue (*30*). This value is in agreement with the estimate obtained in the dog study by comparing the K_dV_R value found in vivo by PET (0.072 ± 0.021 pmole/ml tissue) with the K_d value from the in vitro method (0.49 ± 0.06 pmole/ml tissue), which led to a V_R value equal to 0.147 ml/ml (*1*). A third estimate of this parameter can be obtained by assuming that exchanges between plasma and free ligand compartments were passive transfers. In this case, the two parameters p and k can be assumed to be equal and V_R is deduced from the pV_R-to-k ratio. From the parameter values given in Table 2, V_R is estimated by this method at 0.148 ml/ml. The three estimates of V_R are close to 0.15 ml/ml. By using this value, the equilibrium dissociation constant K_d is evaluated at 2.0 ± 0.5 pmole/ml tissue.

The existence of an irreversible and nonspecific binding process (parameter k_{ns}) was previously shown in dogs since a small part of the binding was not displaced by a large excess of cold MQNB and appeared irreversible during the experiments (*1*). In fact, this nonspecific binding is probably spontaneously reversible with a low rate constant not identifiable from PET data because of the short period of ^{11}C. Moreover, in humans, a large amount of unlabeled MQNB should be avoided, and therefore estimation of this parameter and information about possible irreversibility of nonspecific binding are more difficult to obtain. Assuming,

however, this apparent irreversibility during the experiments, the parameter k_{ns} was estimated using a double-displacement protocol. The two values (0.029 and 0.033 min^{-1}) were comparable to the corresponding parameter in dogs (0.046 ± 0.009 min^{-1}) (*1*). Simulations showed that the percentage of nonspecific binding is low. Therefore, the effect of an individual variation of k_{ns} is weak and, in practice, the k_{ns} estimate from the double-displacement protocol can be used as a constant parameter not subjected to individual variations. Even when k_{ns} was assumed to be null, modification of the parameter estimates was not significant, considering the standard deviations with the three-injection protocol shown in Table 3. The influence of k_{ns} was further reduced with the coinjection protocol because the injected unlabeled ligand dose and thus receptor occupancy and free ligand concentration were decreased: B'_{max} was estimated to be 22 ± 6 pmole/ml tissue with nonspecific correction and 26 ± 7 pmole/ml without correction. This estimation of irreversible nonspecific binding does not give any information about possible nonspecific and reversible binding. It is well known that the modeling approach with PET data is not sensitive enough to detect possible nonspecific and reversible binding reactions with association-dissociation kinetic rate constants much larger than the other compartmental rate constants. Such nonspecific binding is usually located in the free ligand compartment (*31,32*).

The transfer coefficient $k_{+1}/V_R\ B'_{max}$, denoted by most authors as k_3, was calculated to be 34 min^{-1}, which implies rapid binding. After the first labeled injection, the mean residence time in the free ligand compartment was only several seconds and the probability of specific MQNB binding to free receptor sites (defined by $k_3/(k_3 + k + k_{ns})$) was equal to 94%.

The dissociation rate constant (parameter k_{-1}) was estimated to be 0.34 ± 0.08 min^{-1}, a value similar to that found in dogs (0.27 ± 0.03 min^{-1}) (*1*). This value indicates that at any given time about 34% of specifically bound ligand dissociated each minute, a far from negligible amount. However, simple visual inspection of the uptake curves showed a plateau a few minutes after injection of ^{11}C-MQNB, which could be interpreted as irreversible binding (Figs. 3 and 6). In fact, a dissociated ligand molecule still had a probability of 94% binding and thus the apparent dissociation rate is only 0.02 min^{-1} (6% of 0.34 min^{-1}), which explains the curve's plateau. Thus, although MQNB binds to the muscarinic receptor with a high affinity, our results show that it can clearly dissociate from receptor sites, and once it is in the free ligand compartment, there is a much higher probability of the ligand rebinding to the same or another free receptor site than escaping into capillary blood. This high probability of rebinding could be due to the distribution of receptors in clusters at synapses (*24*).

CONCLUSION

In vivo PET measurements allow the measurement of binding parameters in "physiological" conditions. The present results show that it is now possible to quantify myocardial muscarinic receptors in the human heart noninvasively using PET with a simplified protocol by starting with a tracer injection of ^{11}C-MQNB followed 30 min later by coinjection of labeled and unlabeled MQNB.

K_d, however, is not accurately estimated from this protocol, which was optimized in this study for B_{max} identification. In vitro animal studies have shown the possibility of significant changes in affinity constants in pharmacological conditions (*10,33–35*). A good estimation of K_d implies optimizing the two-injection protocol for better estimation of this parameter or using the three-injection protocol, which is longer but well tolerated. It seems reasonable to begin with the three-injection protocol in the exploration of a pathological condition when the pattern of receptor abnormalities is not known. Because these protocols are completely noninvasive, it becomes feasible to investigate possible changes in receptor density and/or affinity in patients.

ACKNOWLEDGMENTS

The authors thank the cyclotron and radiochemistry staff of the Service Hospitalier Frédéric Joliot and D. Raffel, R. Trebossen, B. Verrey, O. Lamer, D. Fournier, F. Hinnen, N. Boullais and M. Crouzel for technical assistance. This work was supported in part by a grant from Lederle Laboratory.

REFERENCES

1. Delforge J, Janier M, Syrota A, et al. Noninvasive quantification of muscarinic receptors in vivo with positron emission tomography in the dog heart. *Circulation* 1990;82:1494–1504.
2. Motulsky HJ. PET receptors: counting receptors using positron emission tomography. *Circulation* 1990;82:1536–1538.
3. Mukherjee A, Wong TM, Buja LM, Lefkowitz RJ. Beta adrenergic and muscarinic cholinergic receptors in canine myocardium: effects of ischemia. *J Clin Invest* 1979;64:1423–1428.
4. Mirro MJ, Manalan AS, Bailey JC, Watanabe AM. Anticholinergic effects of disopyramide and quinidine on guinea pig myocardium mediation by direct muscarinic receptor blockade. *Circ Res* 1980;47:855–865.
5. Robberecht P, Waelbroeck M, Claeys M, Nguyen Huu A, Chatelain P, Christophe J. Rat cardiac muscarinic receptors. II. Influence of thyroid status and cardiac hypertrophy. *Mol Pharmacol* 1982;21:589–593.
6. Pelc LR, Gross GJ, Warltier DC. Changes in regional myocardial perfusion by muscarinic receptor subtypes in dog. *Cardiovasc Res* 1986;20:482–489.
7. Vatner DE, Lee DL, Schwarz KR, et al. Impaired cardiac muscarinic receptor function in dogs with heart failure. *J Clin Invest* 1988;81:1836–1842.
8. Carrier GO, Aronstam RS. Altered muscarinic receptor properties and function in the heart diabetes. *J Pharmacol Exp Ther* 1987;242:531–535.
9. Sharkey J, Ritz MC, Schenden JA, Hanson RC, Kuhar MJ. Cocaine inhibits muscarinic cholinergic receptors in heart and brain. *J Pharmacol Exp Ther* 1988;246:1048–1052.
10. Klangkalya B, Chan A. The effects of ovarian hormones on beta-adrenergic and muscarinic receptors in rat heart. *Life Sci* 1988;42:2307–2314.
11. Brown JH, ed. *The muscarinic receptors.* Clifton: The Humuna Press; 1989.
12. Nathanson NM. Molecular properties of the muscarinic acetycholine receptor. *Ann Rev Neurosci* 1987;10:195–236.
13. Fields JZ, Roeske WR, Morkin E, Yamamura HI. Cardiac muscarinic cholinergic receptors. Biochemical identification and characterization. *J Biol Chem* 1978;253:3251–3258.
14. Wei JW, Sulakhe PV. Regional and subcellular distribution of myocardial muscarinic cholinergic receptors. *Eur J Pharmacol* 1978;52:235–238.
15. Gibson RE, Eckelman WC, Vieras F, Reba RC. The distribution of the muscarinic acetylcholine receptor antagonist, quinuclidinyl benzilate, and quinuclidinyl benzilate methiodide (both tritiated) in rat, guinea pig and rabbit. *J Nucl Med* 1979;20:865–870.
16. Watson M, Yamamura HI, Roeske WR. ^{3}H-Pirenzepine and (−)-^{3}H-quinu-

clidinyl benzilate binding to rat cerebral cortical and cardiac muscarinic cholinergic sites. I. Characterization and regulation of agonist binding to putative muscarinic subtypes. *J Pharmacol Exp Ther* 1986;237:411–418.
17. Syrota A. Receptor binding studies of the living heart. *New Concepts Cardiac Imag* 1988;4:141–166.
18. Syrota A. Positron emission tomography: evaluation of cardiac receptors. In: Marcus ML, Skorton DJ, Schelbert HR, Wolf GL, eds., Braunwald E, consulting ed. *Cardiac imaging—principles and practice: a companion of Braunwald's heart disease.* Philadelphia: W. B. Saunders; 1990:1256–1270.
19. Mazière M, Comar D, Godot J, Collard P, Cepeda P, Naquet R. In vivo characterization of myocardium muscarinic receptors by positron emission tomography. *Life Sci* 1981;29:2391–2397.
20. Syrota A, Comar D, Paillotin G, et al. Muscarinic cholinergic receptor in the human heart evidenced under physiological conditions by positron emission tomography. *Proc Natl Acad Sci USA* 1985;82:584–588.
21. Delforge J, Syrota A, Mazoyer BM. Identifiability analysis and parameter identification of an in vivo ligand-receptor model from PET data. *IEEE Trans Biomed Eng* 1990;37:653–661.
22. Delforge J, Syrota A, Mazoyer BM. Experimental design optimization: theory and application to estimation of receptor model parameters using dynamic positron emission tomography. *Phys Med Biol* 1989;34:419–435.
23. Trebossen R, Mazoyer B. Count rate performances of TTV03: the CEA-LETI time-of-flight positron emission tomograph. *IEEE Trans Med Imaging* 1991;10:261–266.
24. Syrota A, Paillotin G, Davy JM, Aumont MC. Kinetics of in vivo binding of antagonist to muscarinic cholinergic receptor in the human heart studied by positron emission tomography. *Life Sci* 1984;35:937–945.
25. Carson ER. Parameter estimation on positron emission tomography. In: *Positron emission tomography and autoradiography: principle and application for the brain and heart.* New York: Raven Press; 1986:347–390.
26. Patlak CS, Blasberg RG, Fenstermacher JD. Graphical evaluation of blood-to-brain transfer constant from multiple-time uptake data. *J Cereb Blood Flow Metab* 1983;3:1–7.
27. Charbonneau P, Syrota A, Crouzel C, Vallois JM, Prenant C, Crouzel M. Peripheral-type benzodiazepine receptors in the living heart characterized by positron emission tomography. *Circulation* 1986;73:476–483.
28. Vatner DE, Vatner SF, Fujii AM, Homcy CJ. Loss of high affinity cardiac beta adrenergic receptors in dogs with heart failure. *J Clin Invest* 1985;76: 2259–2264.
29. Böhm M, Gierschik P, Jakobs KH, et al. Increase of Giα in human hearts with dilated but not ischemic cardiomyopathy. *Circulation* 82:1249–1265.
30. Walker JL. Intracellular inorganic ions in cardiac tissue. In: Fozzard H, Haber E, Jennings R, Katz AM, Morgan HE, eds. *The heart and cardiovascular system, scientific foundations*. New York: Raven Press; 1986:561–572.
31. Perlmutter JS, Larson KB, Raichle ME, et al. Strategies for in vivo measurement of receptor binding using positron emission tomography. *J Cereb Blood Flow Metab* 1986;6:154–169.
32. Huang SH, Barrio JB, Phelps ME. Neuroreceptor assay with positron emission tomography: equilibrium versus dynamic approaches. *J Cereb Blood Flow Metab* 1986;6:515–521.
33. Sugai Y, Sugai T, Okuda C, Miyazaki M. The interaction of pancuronium and vecuronium with cardiac muscarinic receptors. *Acta Anaesthesiol Scand* 1987;31:224–226.
34. Buxton I, Rozansky D, Brunton L, Motulsky H. Effect of Na^+ on the muscarinic cholinergic receptors of rat ventricular myocytes. *J Cardiovasc Pharmacol* 1985;7:476–481.
35. Tucek S, Musilkova J, Nedona J, Proska J, Shelkovnikow S, Vorcilek J. Positive cooperativity in the binding of alcuronium and N. methylscopolamine to muscarinic acetylcholine receptors. *Mol Pharmacol* 1990;38:674–680.